JOURNAL OF Materials CHEMISTRY

Effect of doping metals on the kinetics of interaction of SnO_2 thin films with oxygen

O. V. Safonova,[a] M. N. Rumyantseva,[a] M. Labeau[b] and A. M. Gaskov*[a]

[a]*Department of Chemistry, Moscow State University, Moscow, 119899 Russia*
[b]*Laboratoire des Materiaux et du Genie Physique, CNRS UMR 5628, Institut National Polytechnique de Grenoble, BP 46, 38402 Saint Martin d'Heres Cedex, France*

The effect of changing the doping metal ($M = Cu$, Ni, Pd, Pt) on the kinetics of oxygen exchange reactions of polycrystalline SnO_2 thin films with gaseous oxygen was studied *in situ* by conductance measurements. It was found that preliminary annealing of SnO_2-based materials in inert (N_2) and active (100 ppm H_2S in N_2) atmospheres affects the kinetics of their reaction with oxygen. Two kinetic models describing the interactions of semiconducting porous materials with gases, *i.e.*, diffusion and surface chemical reactions, are considered.

Introduction

Gas adsorption and surface chemical reactions are of primary importance in solid–gas interaction phenomena. In semiconducting oxides chemisorption of oxygen from air occurs *via* reaction (1):

$$O_2(g) + 2e^- = 2O^-(s) \qquad (1)$$

with a localisation of electrons and formation of an electron-depletion space-charge layer, resulting in low conductance[1–3] [in eqn. (1), (g) and (s) mean gas phase and surface, respectively].

Reducing gases interact with adsorbed oxygen, supply electrons to the conduction band, and the conductance increases:[4]

$$R(g) + O^-(s) = RO + e^-$$

In inert gases, for example N_2, the conductance increases due to the decrease in concentration of surface oxygen [reverse of reaction (1)].

The high sensitivity of the electrical properties of polycrystalline semiconductor oxides to the presence of specific gas molecules is mainly responsible for the development of solid state gas sensors which gained recent prominence due to their low cost, low power consumption, and the possibility of direct connection to standard electronic circuits. Usually the sensor parameters of materials are estimated from plots of the electrical conductance change during the full cycle, including the increase of conductance in reducing gases [response process, eqn. (2)] and the return of conductance in air to the initial value [recovery process, eqn. (1)]. Most of the studies are dedicated to the investigation of the former stage of solid–gas interaction,[5–7] but for the gas sensor applications the recovery process is no less important than the response process.

The dynamic properties of polycrystalline semiconducting oxide materials, *i.e.* response time, and recovery time, are affected by various material properties such as bulk and surface composition, real microstructure, and surface morphology.[8] It was found that the doping metals have especially strong effects on the kinetics of the solid–gas interaction.

In this work, we studied the action of different doping metals ($M = Cu$, Ni, Pd, Pt) on the kinetics and mechanism of interaction of SnO_2 thin films with oxygen (*i.e.*, on the recovery rate). The study was carried out for two cases, which differed in preliminary annealing of the films: either in N_2, or in $H_2S + N_2$ (100 ppm H_2S in N_2). In the first case, all the specific surface reactions were eliminated, with the exception of the oxygen adsorption *via* reaction (1). In the second case, depending on the film composition, different reactions could take place. Thin films of pure and doped tin dioxide were synthesised by pyrosol spraying and magnetron sputtering deposition. The kinetics of the change of electrical conductance in oxygen atmosphere was measured *in situ* in an automatic set-up after preliminary annealing in inert (N_2) and active ($H_2S + N_2$) atmospheres. The kinetic models, limited by diffusion and surface chemical reactions, were used to explain the results observed.

Theoretical model

It is suggested that the conductance of polycrystalline semiconductor materials is mainly determined by the electrical properties of the grain boundaries, affected by chemisorbed gas molecules diffusing through the pores. Intragrain diffusion is ignored because its rate is negligible as compared with that of surface diffusion across the pores.[8]

Assuming that the semiconductor layer is macroscopically homogeneous and adsorption sites are uniformly distributed across the film on pore surfaces, Gardner[6] suggested the following expression for the electrical conductance, G, of the film:

$$G = \frac{\mu\, el}{\pi} \int_0^{x0} n \left(x^2 + \frac{w^2}{4} \right)^{-0.5} \mathrm{d}x \qquad (3a)$$

where e is the electron charge, n is the concentration of free charge carriers, μ is their mobility, and x_0, l, w are the geometrical parameters of the sample (Fig. 1).

We considered the case when $x_0 \ll w$ and $x_0 \ll l$,

$$G = \frac{2\mu\, el}{\pi w} \int_0^{x0} n\mathrm{d}x \qquad (3b)$$

If the material is interacting with a gas, the conductance can change in the same fashion as the concentration of charge carriers n; n depends on time and the coordinate x: $n = n(t,x)$.

In air, the adsorption of oxygen according to reaction (1) results in a decrease of the carrier number n in direct proportion to the concentration of unoccupied adsorption sites c on the pore surfaces. Then,

$$G' = \frac{G - G_\infty}{G_0 - G_\infty} = \frac{\displaystyle\int_0^{x0} (c - c_\infty)\mathrm{d}x}{\displaystyle\int_0^{x0} (c_0 - c_\infty)\mathrm{d}x} = \frac{1}{x_0} \int_0^{x0} c'\mathrm{d}x \qquad (4)$$

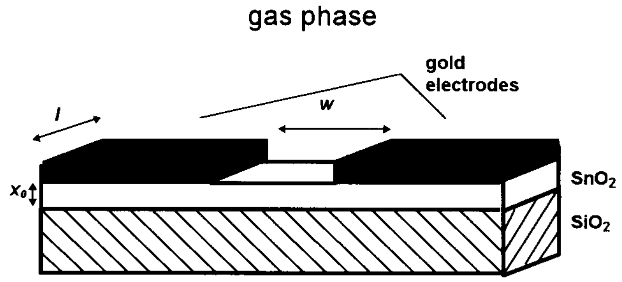

Fig. 1 Scheme of a sensor sample

where

$$c' = \frac{c - c_\infty}{c_0 - c_\infty}$$

Here, G_0 is the initial conductance value before the introduction of O_2 into the system, G_∞ is the steady-state conductance in O_2, G' is the normalised value of conductance, and c_0 and c_∞ are the concentrations of unoccupied adsorption sites initially and when the reaction reaches a steady-state, respectively.

The transient process of conductance change with the gas phase is rather complex, and as a first order approximation, can be modelled by several successive stages: adsorption, diffusion of gas to the outer surface and in the bulk of a porous solid sample, and chemical reactions on the surface. We consider the two simplest cases of the interactions of a SnO_2 film with oxygen.

In the first case, the limiting stage is the linear diffusion of oxygen into the porous film in direction x. The oxygen adsorption results in a decrease of the concentration of unoccupied adsorption sites c at the grain boundaries.[6] This case is equivalent to the diffusion from both sides of a layer of finite thickness $2x_0$.[9] Fick's equation for a SnO_2 layer can be given as:

$$\frac{\partial c'}{\partial t} = D \frac{\partial^2 c'}{\partial x^2}$$

with the boundary conditions:

$$c' = 1,\ 0 < x < 2x_0,\ t = 0;\quad c' = 0,\ x = 2x_0,\ x = 0,\ t > 0 \qquad (5)$$

where D is the oxygen diffusion coefficient.

The solution is the following series:[9]

$$c'(x,t) = \frac{4}{\pi} \sum_{j=0}^{\infty} \frac{1}{2j+1} \exp\left(\frac{-(2j+1)^2\pi^2 Dt}{4x_0^2}\right) \sin\left(\frac{(2j+1)\pi x}{2x_0}\right) \qquad (6)$$

By substituting series (6) into eqn. (4), we obtain for G':

$$G' = \frac{8}{\pi^2} \sum_{j=0}^{\infty} \frac{1}{(2j+1)^2} \exp\left(\frac{-(2j+1)^2\pi^2 Dt}{4x_0^2}\right) \qquad (7)$$

The first term of the above series is a good approximation of eqn. (7):

$$G'(1) = \frac{8}{\pi^2} \exp\left(\frac{-\pi^2 Dt}{4x_0^2}\right) \qquad (8)$$

(strictly speaking at $G' \leqslant 0.8$).[9]

The time dependence of $G'(1)$ is exponential. We designate the x_0-dependent coefficient as k_{dif}, which will be estimated from experimental data as a kinetic coefficient:

$$k_{dif} = \frac{\pi^2 D}{4x_0^2} \qquad (9)$$

In the second case, the transient process is limited by surface reactions of the material with oxygen. Let us assume that the kinetics is described by the equation of the first order reaction:

$$c'(t) = \exp(-k_r t) \qquad (10)$$

where k_r is the rate constant of the reaction.

Substituting eqn. (10) into eqn. (4), we obtain:

$$G' = \exp(-k_r t) \qquad (11)$$

As is seen from eqn. (8) and (11), in both cases the time dependences of G' are the same, within the limits of precision of the coefficients. However, in the case of diffusion model, k_{dif} depends on the film thickness x_0 [eqn. (8)], while in the surface reaction model k_r is independent of it [eqn. (11)]. Therefore, we can write

$$G' = A \exp(-kt) \qquad (12)$$

where k is the effective rate constant corresponding to the recovery process of the sensor materials in oxygen. The value of the effective rate constant k can be estimated from the experimental G *vs.* t data. The analysis of this parameter for films of different thickness x_0 will be applied to elucidate the limiting stage of the recovery process: diffusion or surface reaction.

Experimental

Thin films of pure and doped SnO_2 were obtained on the oxidized single crystal silicon Si $\langle 100 \rangle$ substrates by magnetron sputtering (MS) of metals with subsequent oxidation and pyrosol spraying (PS) deposition.

Tin films of different thickness were deposited by MS at the room temperature. The MS conditions were: Ar pressure $(2\text{–}3) \times 10^{-2}$ Torr, voltage 500 V, target–substrate distance 6 cm. Metallic films were oxidized by annealing in dry air at temperatures of 160 °C (6 h), 300 °C (6 h) and 500 °C (17 h). SnO_2 and $SnO_2(M)$ (M = Cu, Ni, Pd, Pt) films were grown at 490 °C by pyrolysis of an aerosol generated by ultrasound from organic precursor solutions.[10] The precursors used were: dibutyltin diacetate, copper trifluoroacetylacetonate, nickel ethyl hexanoate, palladium acetylacetonate and platinum acetylacetonate.

The film thicknesses were measured by Talystep profilometry and scanning electron microscopy (SEM). The concentration of admixtures was determined by electron probe microanalysis (EPMA). The average size of SnO_2 crystallites calculated from X-ray diffraction (XRD) by using the Debye–Scherrer equation varied from 5 to 10 nm. Fig. 2 shows the surface patterns

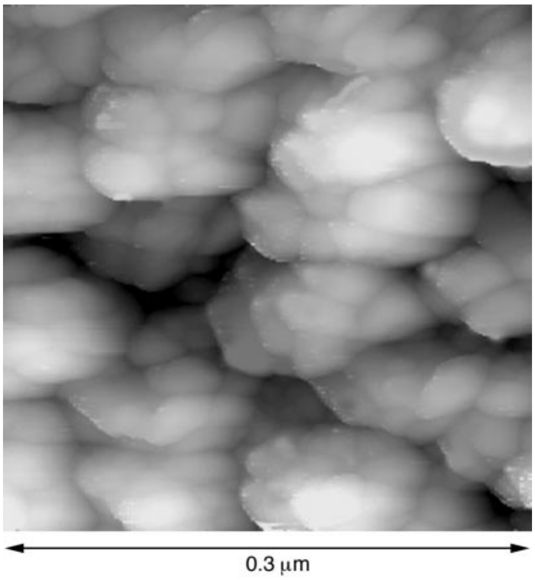

Fig. 2 AFM image of the surface of SnO_2 film

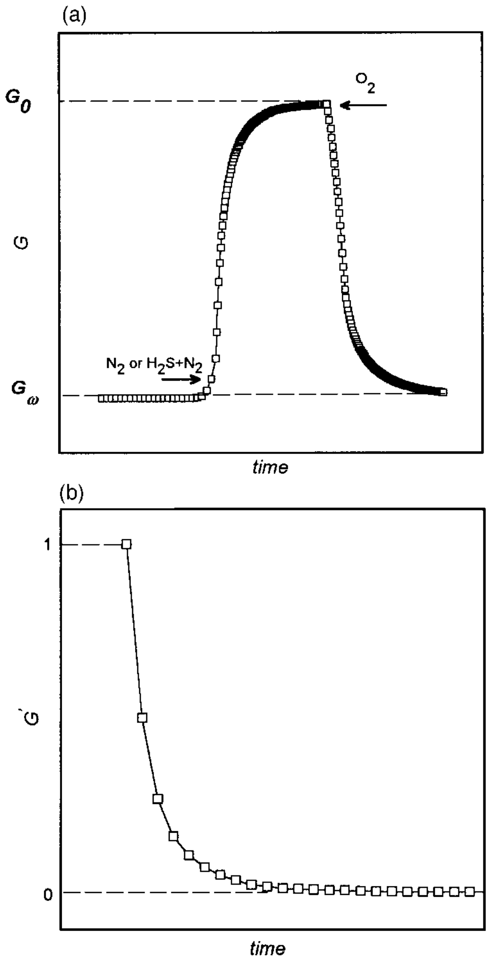

Fig. 3 Schematic time dependences of (a) G and (b) G'

Table 1 Characteristics of synthesized films

films	concentration of doping metal (atom%)	synthesis method	x_0/μm
$SnO_2(1)$	—	MS	0.2
$SnO_2(2)$	—	MS	0.8
$SnO_2(3)$	—	MS	1.0
SnO_2	—	PS	1.0
$SnO_2(Cu)$	0.7	PS	1.0
$SnO_2(Ni)$	0.7	PS	1.0
$SnO_2(Pd)$	1.2	PS	1.0
$SnO_2(Pt)$	0.6	PS	1.0

obtained by the atomic force microscopy (AFM) technique. Despite the differences in the synthesis procedures, the surface relief was practically the same in each case. It was demonstrated that all the samples have a porous structure and SnO_2 grains are combined into aggregates with an average size of about 0.1 μm. The sample properties are listed in Table 1.

The contacts were pressed on thin gold films with the constant geometric parameters: $w=3$ mm, $l=5$ mm. The measurements of electric current proportional to the conductance value were performed in dc mode at the fixed voltage $U=1$ V. All the films were preliminary annealed either in inert media (N_2) or in a reducing atmosphere of H_2S+N_2 (100 ppm H_2S in N_2). The annealing duration was 240 min. The conductance transients when the materials were exposed to gases were investigated with a programmed set-up at a fixed temperature in the interval from 130 to 280 °C. Fig. 3(a) illustrates a typical conductance transient curve in N_2 or H_2S+N_2 atmosphere (response) and in oxygen (recovery). Fig. 3(b) shows the normalised value of conductance G' corresponding to eqn. (4). G' *vs.* t curves calculated from experimental data for all films and different temperatures were used to estimate the effective rate constant k [eqn. (12)].

Table 2 Value of the effective rate constant k for SnO_2 films of different thickness [thickness of $SnO_2(1)=0.2$, $SnO_2(2)=0.8$, $SnO_2(3)=1.0$ μm]

T/°C	$SnO_2(1)$ $k\times10^4$/s^{-1}	$SnO_2(2)$ $k\times10^4$/s^{-1}	$SnO_2(3)$ $k\times10^4$/s^{-1}
180	5.8	6.2	7.0
200	7.0	5.8	7.2
230	6.8	7.5	7.5

Results and Discussion

Table 2 presents k values for pure SnO_2 films of different thickness ($x_0=0.2$, 0.8, 1.0 μm) obtained in O_2 after annealing in N_2. It was found that the process rate constant did not increase with decreasing of film thickness. Within the chosen theoretical model [eqn. (12)] the error of the estimation is greater than the differences in k values obtained for films of different thickness. Hence, the mechanism of the recovery process can be represented as a quick linear diffusion of oxygen into a porous sample, followed by a slow surface reaction. In subsequent work we used SnO_2 and $SnO_2(M)$ (M = Cu, Ni, Pd, Pt) films of the same thickness, 1.0 μm (Table 1).

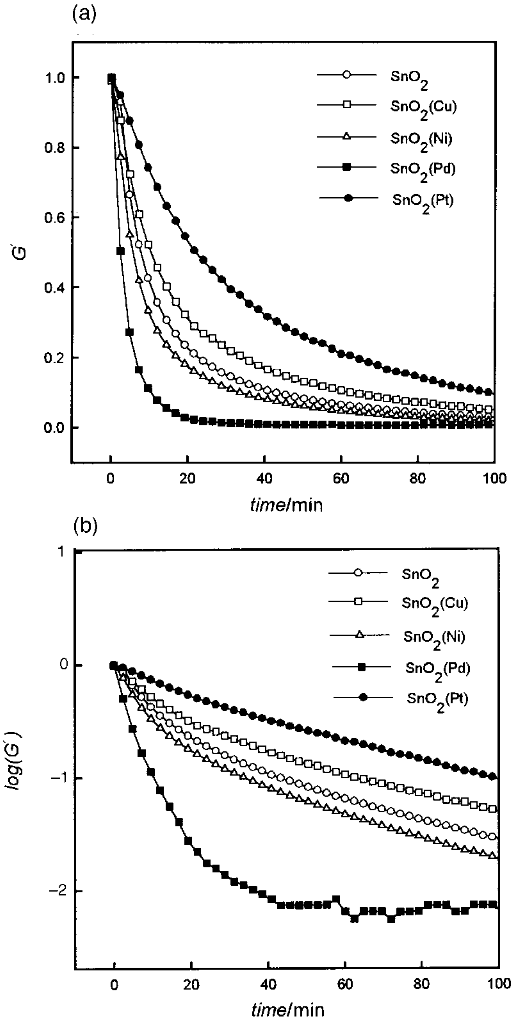

Fig. 4 Experimental time dependences of (a) G' and (b) log G' for SnO_2 and $SnO_2(M)$ (M = Cu, Ni, Pd, Pt) films in the N_2–O_2 system at 250 °C

Table 3 Values of the effective rate constants k, k_1, k_2 for SnO_2, $SnO_2(Cu)$, $SnO_2(Ni)$, $SnO_2(Pd)$, $SnO_2(Pt)$ films in N_2–O_2 and H_2S–O_2 systems

T/°C	SnO_2 $k\times10^4$/s^{-1}	$SnO_2(Cu)$ $k\times10^4$/s^{-1}		$SnO_2(Ni)$ $k\times10^4$/s^{-1}		$SnO_2(Pd)$ $k_1\times10^4$/s^{-1}	$SnO_2(Pd)$ $k_2\times10^4$/s^{-1}	$SnO_2(Pt)$ $k\times10^4$/s^{-1}
(a) Rate constants in N_2–O_2 system:								
180	5.8	5.3		7.7		8.3	4	3.8
230	7.2	5.8		8.8		18	5.3	5.2
250	8.5	7.5		10		25	7.5	5.0
280	13	10		18		35	8.3	5.3
		$k_1\times10^4$/s^{-1}	$k_2\times10^4$/s^{-1}	$k_1\times10^4$/s^{-1}	$k_2\times10^4$/s^{-1}			
(b) Rate constants in H_2S–O_2 system:								
180	4.5	200	3.8	53	3.8	12	3.6	3.3
200	6.5	210	4.0	55	5.2	17	5.7	3.8
230	6.8	230	4.5	58	7.5	23	6.8	5.2

We studied the kinetics of oxygen exchange in the absence of reducing gases. The system N_2–O_2 was chosen as the model one. Fig. 4(a) shows the experimental G' *vs.* t dependences in O_2 after preliminary annealing of samples in N_2. The film doped with palladium demonstrates the fastest recovery rate. The same data in logarithmic coordinates [Fig. 4(b)] were used for determination of the k values. Experimental data obtained for SnO_2 and $SnO_2(M)$ (M = Cu, Ni, Pd, Pt) films give close values of the rate constant k (Table 3). For a $SnO_2(Pd)$ film we can distinguish two regions on the log G' *vs.* t dependences: the initial region with the rate constant k_1, and the final region with the rate constant k_2. The rate of oxygen exchange in the final region is close to that for the undoped SnO_2 sample. The strong effect of palladium on the kinetics of oxygen exchange can be explained by the change of the Pd oxidation state within the framework of the electronic mechanism discussed in the literature.[8,11] In oxygen atmosphere, palladium on the surface of SnO_2 grains exists in the form of PdO which acts as an electron acceptor in polycrystalline tin dioxide. This results in growth of the depletion layer in SnO_2, and the conductance decreases. In an inert gas atmosphere (N_2), lacking oxygen, PdO transforms into Pd metallic clusters. The electronic effect of PdO vanishes and the tin dioxide conductance increases again. Pt, Cu and Ni, apparently, do not change their oxidation states under given conditions.[8] This is why their effect on the kinetics of the SnO_2 recovery processes is weak.

Fig. 5(a) and (b) show G' *vs.* t and log G' *vs.* t dependences measured in O_2 after preliminary annealing of samples in H_2S+N_2 (H_2S–O_2 system) for the same films. In this case, $SnO_2(Cu)$ and $SnO_2(Ni)$ films display the fastest recovery rate. For $SnO_2(Cu)$ and $SnO_2(Ni)$ in Fig. 5(b), we also can single out two regions: the initial, fast region, and the final, slow region. The rate of the recovery process in the final region is close to that for undoped SnO_2. The temperature dependences of k, k_1, and k_2 for these films are presented in Table 3.

The important effect of copper and nickel on the recovery process in these experiments can be explained by the selective chemical reactions of CuO and NiO with H_2S.[8,12] For the $SnO_2(Cu)$ system the electron-barrier mechanism is assumed. In O_2 atmosphere, copper on the surface of SnO_2 grains is in the form of CuO, which is a p-type semiconductor. On the SnO_2–CuO interface the p–n junction takes place, which is destroyed in hydrogen sulfide, because CuO is reversibly transformed into CuS, a substance which exhibits metallic conduction. In the case of $SnO_2(Ni)$, the mechanism also supposes the selective reactions of NiO (p-type semiconductor) with formation of nickel sulfides. However, this process is inhibited due to the fact that Ni is incorporated into the SnO_2 lattice.[12]

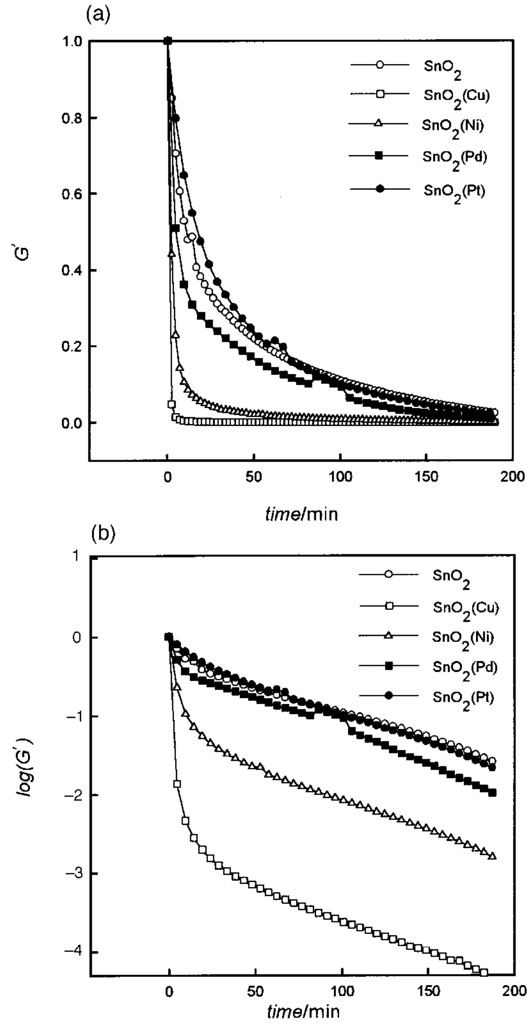

Fig. 5 Experimental time dependences of (a) G' and (b) log G' for SnO_2 and $SnO_2(M)$ (M = Cu, Ni, Pd, Pt) films in the H_2S/O_2 system at 180 °C

The values of k, k_1, and k_2 for SnO_2, $SnO_2(Pd)$ and $SnO_2(Pt)$ films are independent of the preliminary annealing conditions (N_2 or H_2S+N_2) (Table 3). In contrast, $SnO_2(Cu)$ and $SnO_2(Ni)$, after being annealed in H_2S+N_2, display values of k_1 which are two orders of magnitude greater than k values for the films annealed in N_2. Thus, the mechanism of barrier switching in SnO_2–CuO and SnO_2–NiO systems as a function of gas phase composition ensures a faster rate of recovery than that of a simple mechanism of oxygen adsorption *via* reaction (1).

As has been already mentioned, for some films two regions can be distinguished in plots of log G' *vs.* t: the initial, fast and the final, slow regions. The rate in the final region is close to that of the oxygen reaction with an undoped SnO_2 sample. To explain this fact, we propose the following phenomenological model. We assign the initial region G_1 to reactions on the intergrain junctions SnO_2–CuO, SnO_2–NiO or SnO_2–PdO,

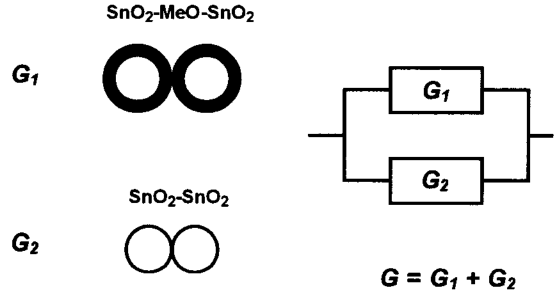

Fig. 6 The model of conductance of SnO_2 films doped with metals

and the final region G_2 to the interaction of oxygen with SnO_2 grains. If these two processes are parallel, then the integral conductance of the doped sample can be determined by a system of parallel resistors as presented in Fig. 6. Then the conductance G of a SnO_2(Me) film is the sum of the G_1 and G_2 contributions:

$$G = G_1 + G_2 \tag{13}$$

where

$$G_1 = A_1 + B_1 \exp(-k_1 t);\ G_2 = A_2 + B_2 \exp(-k_2 t) \tag{14}$$

With the framework of the model put forward, we can quantitively describe the experimental dependences shown in Fig. 4(b) and 5(b).

Conclusions

The effect of the doping metal (Cu, Ni, Pd, Pt) on the rate of interaction of SnO_2 thin films with oxygen was studied. We have demonstrated that the recovery process is more complicated than merely oxygen adsorption on the grain surface. The kinetics of the recovery process depends on the sample prehistory, *i.e.*, on the gas phase composition during the preliminary annealing. In the case of annealing in the H_2S-containing atmosphere the important role of surface chemical reactions was shown. It was found that copper and nickel have a strong effect on the rate of the recovery process. However, in the absence of preliminary chemical attack, after annealing in nitrogen, SnO_2(Pd) exhibited the highest recovery rate.

Two kinetic models of the recovery process in oxygen for SnO_2-based thin films are considered: the linear diffusion and the surface reaction. The experimental dependences G *vs.* t for the samples of different thickness x_0 are in favour of the surface reaction model.

This work was supported by NATO Linkage grant HTECH.LG 960607. The authors are grateful to M. Gaidi for SnO_2 (Pt) film preparations and to G. Delabouglis for valuable technical assistance.

References

1 G. Heiland, *Sens. Actuators*, 1982, **2**, 343.
2 V. Lantto, P. Romppainen and S. Leppavuori, *Sens. Actuators B*, 1988, **14**, 149.
3 J. McAleer, P. Moseley, J. Norris and D. Williams, *J. Chem. Soc., Faraday Trans.*, 1987, **83**, 1323.
4 D. Kohl, *Sens. Actuators*, 1989, **18**, 71.
5 S. Wlodek, K. Colbow and F. Cansadori, *Sens. Actuators B*, 1991, **3**, 123.
6 J. Gardner, *Semicond. Sci. Technol.*, 1989, **4**, 345.
7 J. Gardner, *Sens. Actuators B*, 1990, **1**, 166.
8 N. Yamazoe, *Sens. Actuators B*, 1991, **5**, 7.
9 P. Shewmon, *Diffusion in Solids*, McGraw Hill Book Company, New York, 1964.
10 M. N. Rumyantseva, A. M. Gaskov, L. I. Ryabova, J. P. Senateur, B. Chenevier and M. Labeau, *Mater. Sci. Eng.*, 1996, **41**, 333.
11 C. Xu, J. Tamaki, N. Miura and N. Yamazoe, *J. Electrochem. Soc.*, 1996, **143**, 148.
12 M. Rumyantseva, M. Labeau, G. Delabouglise, L. Ryabova, I. Kutsenok and A. Gaskov, *J. Mater. Chem.*, 1997, **7**, 1785.

Paper 7/07691F; *Received* 24*th October*, 1997